J. Am. Chem. Soc. **1992**, *114*, 6505–6512

Plasma-Induced Free Radicals of Polycrystalline *myo*-Inositol Studied by Electron Spin Resonance. Orbital Rehybridization-Induced Effect of Hydroxylalkyl Radicals on Their Reactivities in Crystalline State[†,1]

Masayuki Kuzuya,* Nahoko Noda, Shin-ichi Kondo, Kaei Washino, and Akihiro Noguchi

Contribution from the Laboratory of Pharmaceutical Physical Chemistry, Gifu Pharmaceutical University, 5-6-1, Mitahora-higashi, Gifu 502, Japan. *Received October 22, 1991*

Abstract: We report the first detailed ESR study of plasma-induced carbohydrate radicals in powdered *myo*-inositol formed by plasma irradiation followed by temperature annealing. On the basis of the ESR kinetics coupled with the systematic computer simulations, it was found that plasma irradiation produced the hydroxylalkyl radicals at all four possible sites by hydrogen elimination with a preferential formation at C2 and C5. However, a striking difference in the reactivity (stability) of the hydroxylalkyl radicals was observed. The radical at C1(═C3) (**1**) was extremely stable even at 120 °C for 2 h, while the radical at C4(═C6) was very unstable so that it underwent spontaneously the dehydration to give the acylalkyl radical exclusively at C3(═C1) (**4**). We rationalize the observed anomalies in terms of the special conformation of O–H bond at C1(═C3) in crystalline *myo*-inositol, which is the only O–H bond s-trans to the C–H bond with respect to the C–O bond axis. This specific conformation leads to the different reactivity of the hydroxyl group at C1(═C3) induced by an orbital rehybridization from tetrahedral sp^3 carbon to the planar sp^2 carbon on the radical formation. Although this specific interpretation is valid only in a solid when the hydrogen of hydroxyl group is fixed by the hydrogen bonding network, the difference in radical reactivity is a general phenomenon with broad implications for carbohydrate radicals, providing a pioneering concept to facilitate assignment of the carbohydrate radical structure in the crystalline state.

Introduction

A number of electron spin resonance (ESR) studies of stable free radicals generated in a variety of solid state carbohydrates[2] (powder[3] and single crystals[4]) by X-, γ-, and UV-ray radiation have been reported. This reflects, in part, interest in the important physiological roles of these compounds in living systems. Comparison of susceptibility to the radical formation among bioactive carbohydrates is of importance in the radiation damage of DNA including radical-induced cleavage of the sugar phosphate backbone of DNA.[5]

The ESR signals observed in biological systems are best described as powder spectra associated with overlapping spectra of randomly oriented molecules, since the majority of the radicals observed are either in slowly tumbling structures or in rigid media.

In view of the severe broadening of powder spectra due to a small amount of anisotropy in the *g* and/or α-hydrogen hyperfine tensor, as is usually the case for carbon-based organic free radicals, an unambiguous identification of the powder radicals cannot generally be made on the basis of spectroscopic evidence alone.

It has been demonstrated in a certain case[6] that the analysis of powder ENDOR spectrum can also permit radical identification as well as the principal anisotropic parameters of a free radical at a higher level of precision. This approach, however, is not always feasible, particularly when the spectrum contains more than one radical.

Spin trapping techniques have been also applied for a determination of the carbohydrate radicals.[7] However, the radical identification of irradiated carbohydrates is not always of high credibility.[8]

In spite of the frequent difficulty in interpretation of powder spectra, the direct analyses of the spectra could provide fruitful information about the nature of the radicals, if one can carry out the systematic studies including the ESR kinetics coupled with the aid of computer simulations. Such studies, in fact, have recently proven to be equally valid in elucidation of plasma-induced radical structures from the outlines of multicomponent spectra on several kinds of synthetic vinyl polymers.[9]

Several authors have reported the studies on plasma irradiation of several polycarbohydrates.[10,11] But research has so far been directed mainly toward characterization of the surface properties of the plasma-treated materials. The detailed ESR studies on the

---

[†] This paper is dedicated to Professor Harold Hart for the celebration of his 70th birthday.

(1) Part of this work was presented at the Symposium of *Free Radical Reactions of Carbohydrates*; 109th ACS Meeting, Boston, MA, 1990.

(2) Sonntag, C. Free-Radical Reactions of Carbohydrates as Studied by Radiation Techniques. *Advances in Carbohydrate Chemistry and Biochemistry*; Tipson, R. S., Horton, D., Eds.; Academic Press: New York, 1980; Vol. 37, pp 7–77.

(3) (a) Truby, F. K.; Storey, W. H., Jr. *J. Chem. Phys.* **1959**, *31*, 857. (b) Bailey, A. J.; Barker, S. A.; Brimacombe, J. S.; Pooley, D.; Spence, D. H. *Nature* (*London*) **1961**, *190*, 259. (c) Collins, M. A. *Nature* (*London*) **1962**, *193*, 1061. (d) Shields, H.; Hamrich, P. *J. Chem. Phys.* **1962**, *37*, 202. (e) Dilli, S.; Garnett, I. L. *Nature* (*London*) **1963**, *198*, 984. (f) Herak, J. N.; Adamic, K.; Blinc, R. *J. Chem. Phys.* **1965**, *42*, 2388. (g) Lomaglio, G. C. R. *Seances Acad. Sci., Ser. B.* **1967**, *264*, 1637. (h) Baugh, P. J.; Kershaw, K.; Phillips, G. O. *Nature* **1969**, *221*, 1138. (i) Neubacher, H. *Biophysik* **1969**, *6*, 161. (j) Derouane, E. G.; Vendrine, J. V. *Chem. Phys. Lett.* **1974**, *29*, 222. (k) Dizdaroglu, M.; Henneberg, D.; Neuwald, K.; Schomburg, G.; Sonttag, C. *Z. Naturforsch.* **1977**, *32b*, 213.

(4) (a) Ueda, H.; Kuri, Z.; Shida, S. *J. Chem. Phys.* **1961**, *35*, 2145. (b) Ueda, H. *J. Phys. Chem.* **1963**, *67*, 2185. (c) Phillips, G. O. *Radiat. Res. Rev.* **1972**, *3*, 335. (d) Graslund, A.; Lofroth, G. *Acta Chem. Scand., Ser. B* **1975**, *29*, 475. (e) Iwasaki, M.; Toriyama, K. *Chem. Phys. Lett.* **1976**, *41*, 59. (f) Budzinski, E. E.; Potter, W. R.; Potienko, G.; Box, H. C. *J. Chem. Phys.* **1979**, *70*, 5040. (g) Box, H. C.; Budzinski, E. E.; Freund, H. G.; Potter, W. R. *J. Chem. Phys.* **1979**, *70*, 1320. (h) Madden, K. P.; Bernhard, W. A. *J. Phys. Chem.* **1979**, *83*, 2643. (i) Madden, K. P.; Bernhard, W. A. *J. Chem. Phys.* **1979**, *70*, 2431. (j) Madden, K. P.; Bernhard, W. A. *J. Chem. Phys.* **1980**, *72*, 31. (k) Locher, S. E.; Box, H. C. *J. Chem. Phys.* **1980**, *72*, 828. (l) Budzinski, E. E.; Potter, W. R.; Box, H. C. *J. Chem. Phys.* **1980**, *72*, 972. (m) Samskog, P.-O.; Lund, A. *Chem. Phys. Lett.* **1979**, *75*, 525. (n) Samskog, P.-O.; Lund, A.; Nilsson, G.; Symons, M. C. R. *J. Chem. Phys.* **1980**, *73*, 4862. (o) Samskog, P.-O.; Lund, A.; Nilsson, G. *Chem. Phys. Lett.*, **1981**, *79*, 447. (p) Samskog, P.-O.; Kispert, L. D.; Lund, A. *J. Chem. Phys.* **1982**, *77*, 2330. (q) Madden, K. P.; Bernhard, W. A. *J. Phys. Chem.* **1982**, *86*, 4033. (r) Madden, K. P.; Bernhard, W. A. *J. Phys. Chem.* **1982**, *86*, 1712. (s) Box, H. C.; Budzinski, E. E. *J. Chem. Phys.* **1983**, *79*, 4142. (t) Lund, A.; Awadelkarim, O.; Lindgren, M.; Westerling, J. *J. Phys. Chem.* **1986**, *90*, 5584.

(5) See, for example: Ward, J. F. *J. Chem. Ed.* **1981**, *58*, 135.

(6) O'Malley, P. J.; Babcock, G. T. *J. Am. Chem. Soc.* **1986**, *108*, 3995.

(7) Perkins, M. J. Spin Trapping. In *Advances in Physical Organic Chemistry*; Gold, V., Bethell, D., Eds.; Academic Press: New York, 1980; Vol. 17, pp 1–64.

(8) See, for example: Thiey, C. J.; Agnel, J. P. L.; Frejaville, C. M.; Raffi, J. J. *J. Phys. Chem.* **1983**, *87*, 4485.

0002-7863/92/1514-6505$03.00/0

elucidation of the plasma-induced surface radicals have not been worked out, despite the fact that the importance of plasma-induced radicals have often been emphasized for understanding of the nature of plasma treatment.[12]

Elucidation of the structure of radicals formed in one of the polyhydric alcohols, inositol, is of fundamental significance for an initial study of various carbohydrate radicals, because of the suitability as a model for more complicated carbohydrates.

Among the nine possible stereoisomers of inositol, only *myo*-inositol is commercially available and bioactive, being found in living systems as various combined forms such as phosphatidylinositol (one of the phosphaglycerides).

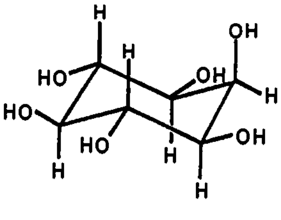

myo-inositol

The ESR study on *myo*-inositol radicals have been reported in aqueous solution produced by the reactions with hydroxyl radicals from the biomimetic Ti(III)–H_2O_2 system[13] and photolysis.[14] Among a number of ESR studies of solid state carbohydrates, however, only X-irradiated single crystalline *myo*-inositol has been investigated in ESR/ENDOR measurements at low temperature.[15] It has been shown that three radicals, one alkoxy radical and two hydroxylalkyl radicals, have been formed.[15a]

One of the advantages of plasma irradiation over other types of high energy radiation for the study of solid state radicals is that the radical formation can be achieved with a brief plasma irradiation by a simple experimental apparatus such as that we have devised.[9c] This method makes it possible not only to study the radicals formed without a significant change of solid morphology but also to follow readily the ESR kinetics for radical formation.

We have undertaken plasma irradiation at room temperature on powdered (polycrystalline) *myo*-inositol followed by temperature annealing, and the radicals formed were studied by ESR with the aid of systematic computer simulations.

Experimental Section

Materials. Powdered (polycrystalline) anhydrous *myo*-inositol was purchased from Nacarai Tesque Co. Ltd (Japan). It was screened with a 100–140 mesh sieve and dried at 70 °C for 6 h in vacuo.

Method of Plasma Irradiation. Powdered samples (100 mg) were placed in a specially designed ampule (30-mm i.d., 100-mm long) connected with a capillary tube (2-mm i.d.) at the uppermost part of the ampule. The ampule was filled with argon gas for plasmolysis (0.3 Torr) and sealed. Then the plasma state was sustained for the prescribed period of time with agitation of samples at room temperature by a radio frequency discharge of inductive coupling at 13.56 MHz with the supplied power (50 W). The ESR measurements were performed while turning the ampule upside down after plasma irradiation at appropriate intervals, which is fundamentally the same procedure as that reported earlier.[9c]

ESR Spectral Measurement. ESR spectra were recorded by a JESRE1X (JEOL) spectrometer with X-band and 100 KHz field modulation. Care was taken to ensure that no saturation occurred and that the line shape was not distorted by excessive modulation amplitude. From a plot of the square root of the microwave power versus the signal peak height, a microwave power level of 0.01 mW was chosen. The ESR spectral intensity was determined by double integration. The radical concentration (spin numbers/g) was calculated from the spectral intensities with the aid of calibrated lines obtained from the spectral intensities of PMMA (polymethylmethacrylate) sample impregnated with DPPH. Measurements of g values were made relative to the fourth signal from the lower magnetic field ($g = 1.981$) of Mn^{2+} in MgO.

Computer Simulation of ESR Spectra. Computer simulations were performed on a 32-bit microcomputer (NEC PC9801RA). The simulated spectra were obtained from Lorentzian functions by fitting iteratively the spectroscopic parameters (g value, line width at half-height, hyperfine splitting constant (HSC), and relative intensity) with the observed digitized spectra using a nonlinear least squares method.[9c] The simulation programs were fabricated so as to include the effect of g factor anisotropy and/or α-hydrogen anisotropy on the line shape of powder spectra according to Kneubühl's equation[16a] and Cochran's equation,[16b] respectively. An anisotropic interaction of β-hydrogens is usually small (less than 0.3 mT) so that such an effect was not considered in the present spectral simulation.

To assist the simulation procedure, we have also fabricated the program for obtaining the difference spectrum by subtracting one observed spectrum from another.

Molecular Orbital Calculations. The molecular orbital calculations were carried out by the UAM1 procedure[17] (AM1 with the UHF formalism[18]) as implemented in the MOPAC program (QCPE, No. 549). Full geometry optimization was started from the standard bond lengths and angles.[19] The calculation was performed on a FACOM 780/20 computer at the Computation Center of Nagoya University.

Results

Observed ESR Spectra of Plasma-Irradiated *myo*-Inositol Followed by Temperature Annealing. Figure 1 shows the progressive changes in the ESR spectra on plasma irradiation at various durations (A), and those on heating of the 15-s plasma-irradiated sample at 120 °C for 2 h (B), and followed by 155 °C for 1.5 h (C).

It is immediately seen from Figure 1A that the spectral pattern has gradually changed with increasing spectral intensity in the course of plasma irradiation, and, after 300-s plasma irradiation, the spectral pattern did not appreciably change on further plasma duration (600 s).

Note that the final ESR spectrum remained also unchanged in both spectral shape and intensity on standing for a long period of time at room temperature, even on exposure to air.

Figure 1B shows a series of spectra when the sample plasma-irradiated for 15 s was heated at 120 °C. It is seen that the spectral pattern gradually changed but differently from the changes in the course of plasma irradiation. Some peaks appear to increase in intensity, while other peaks (such as two independent triplets indicated by arrows in Figure 1B) appear to decay and finally disappeared in 2 h. After that, the spectral pattern did not appreciably change even on prolonged heating at this temperature.

---

(9) (a) Kuzuya, M.; Koide, A.; Ito, A.; Noguchi, A. *Chem. Lett.* **1989**, 555. (b) Kuzuya, M.; Noguchi, A.; Ito, H.; Kondo, S.; Noda, N. *J. Polym. Sci., Polym. Chem.* **1991**, *29*, 1. (c) Kuzuya, M.; Noguchi, A.; Ishikawa, M.; Koide, A.; Sawada, K.; Ito, A.; Noda, N. *J. Phys. Chem.* **1991**, *95*, 2398. (d) Kuzuya, M.; Ito, H.; Kondo, S.; Noda, N.; Noguchi, A. *Macromolecules* **1991**, *24*, 6612. (e) Kuzuya, M.; Kamiya, K.; Sawada, K. *Proc. Jpn. Symp. Plasma Chem.* **1991**, *4*, 317. (f) Kuzuya, M.; Ishikawa, M.; Noguchi, A.; Sawada, K.; Kondo, S. *J. Polym. Sci., Polym. Chem.* **1992**, *30*, 379. (g) Kuzuya, M.; Kondo, S.; Ito, H.; Noguchi, A. *J. Appl. Sur. Sci.*, in press. (h) See, for review: Kuzuya, M. Electron Spin Resonance Study on Solid State Radicals Induced by Plasma Irradiation. In *Trends in Physical Chemistry*; Science Research Integration: India, 1991; Vol. 2, pp 39–63.

(10) Pavlath, A. E. Plasma Treatment of Natural Materials. In *Techniques and Applications of Plasma Chemistry*; Hollahan, J. R., Bell, A. T., Eds.; Wiley: New York, 1974; pp 149–175.

(11) (a) Riccobono, P. X.; Ahmadzai, H.; Bartsch, F. F.; Cate, A. L.; Ferrante, G.; Lee, W. K.; Light, L. L.; Minoff, C.; Roth, P. B. *Text. Chem. Color* **1973**, *5*, 239. (b) Jung, H. Z.; Ward, T. L.; Benerito, R. R. *Text. Res. J.* **1977**, *48*, 217. (c) Ward, T. L.; Jung, H. Z.; Hinojosa, O.; Benerito, R. R. *Surf. Sci.* **1978**, *76*, 257. (d) Ward, T. L.; Zyng, H. Z.; Hinojosa, O.; Benerito, R. R. *J. Appl. Polym. Sci.* **1979**, *23*, 1987. (e) Ward, T. L.; Benerito, R. R. *Polym. Photopolym.* **1983**, *3*, 267.

(12) Hudis, M. Plasma Treatment of Solid Materials. In *Techniques and Applications of Plasma Chemistry*; Hollahan, J. R., Bell, A. T., Eds.; Wiley: New York, 1974; pp 113–147.

(13) (a) Norman, R. O. C.; Pritchett, R. J. *J. Chem. Soc (B)* **1967**, 1329. (b) Gilbert, B. C.; King, D. M.; Thomas, C. B. *J. Chem. Soc., Perkin Trans. 2* **1980**, 1821.

(14) (a) Criddle, W. J. *Nature* **1964**, *201*, 815. (b) Criddle, W. J.; Jones, B.; Ward, E. *Chem. Ind.* **1967**, 1833. (c) Criddle, W. J.; Ward, E. *J. Chem. Soc. (B)* **1970**, 40.

(15) (a) Box, H. C.; Budzinski, E. E. *J. Chem. Phys.* **1977**, *67*, 4726. (b) Budzinski, E. E.; Box, H. C. *J. Chem. Phys.* **1978**, *68*, 5296. (c) Nilsson, G.; Westerling, J.; Lund, A.; Lindgren, M. *J. Chem. Phys.* **1986**, *85*, 2609.

(16) (a) Kneubühl, F. K. *J. Chem. Phys.* **1960**, *33*, 1074. (b) Cochran, E. L.; Adrian, F. J.; Bowers, V. A. *J. Chem. Phys.* **1961**, *34*, 1161.

(17) Dewar, M. J. S.; Zoebisch, E. G.; Healy, F. E.; Stewart, J. J. P. *J. Am. Chem. Soc.* **1985**, *107*, 3902.

(18) Pople, J. A.; Nesbet, R. K. *J. Chem. Phys.* **1954**, *22*, 571.

(19) Pople, J. A.; Beveridge, D. L. *Approximate Molecular Orbital Theory*; McGraw-Hill: New York, 1970; p 111.

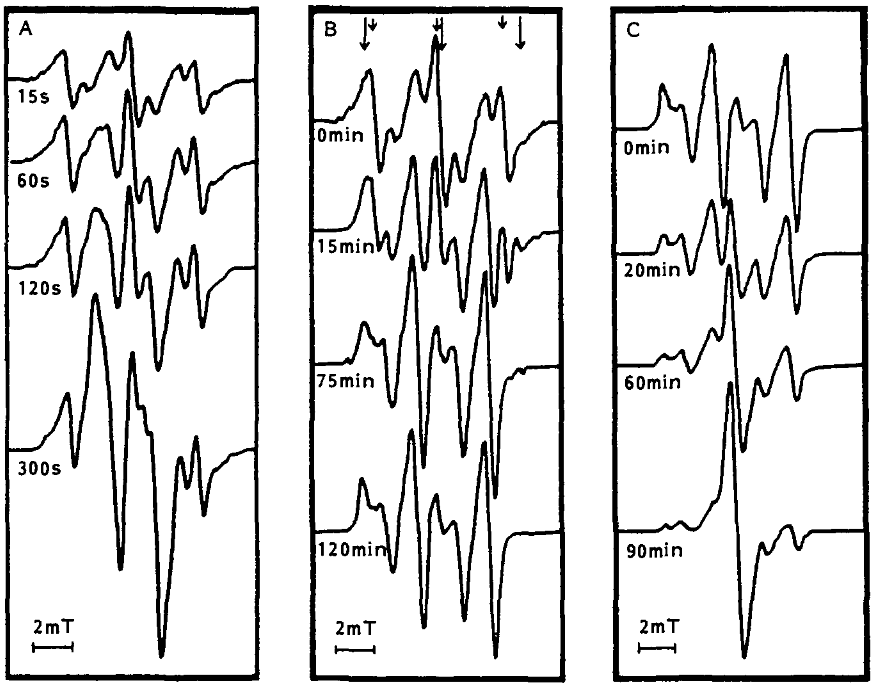

Figure 1. Progressive changes of observed ESR spectra of plasma-irradiated *myo*-inositol as a function of (A) plasma duration, (B) heating at 120 °C of 15-s plasma-irradiated *myo*-inositol, and (C) heating at 155 °C after heating at 120 °C for 2 h.

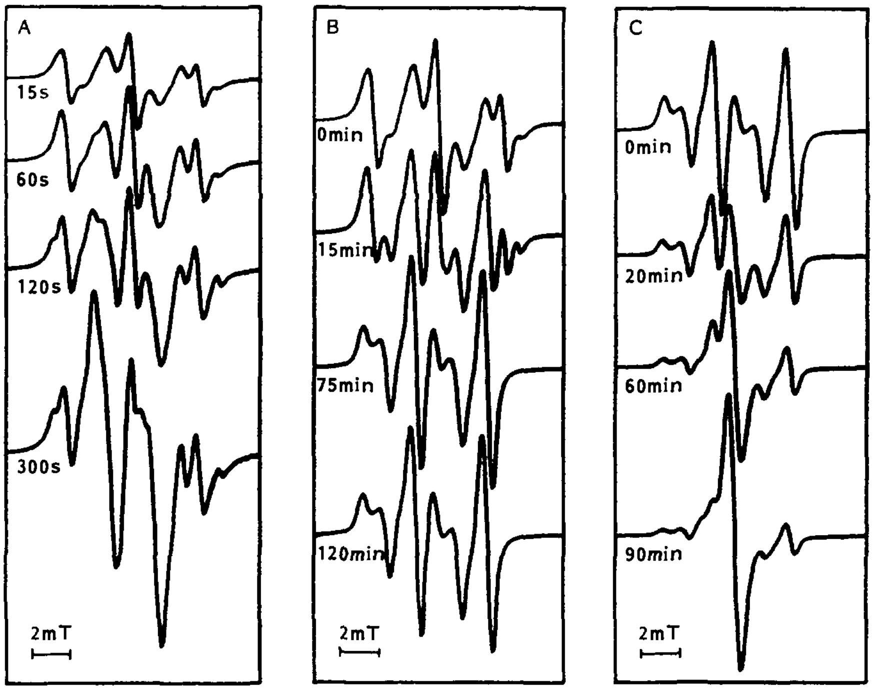

Figure 2. Simulated spectra of plasma-irradiated *myo*-inositol corresponding to Figure 1.

Figure 1C shows the further spectral changes when the temperature was raised up to 155 °C after the heating experiment at 120 °C for 2 h. It can be seen that the spectral pattern started again to change, but differently from those at 120 °C, toward the formation of a single broad line with a small amount of *g* anisotropy.

Simulated Spectra. Since all these observed spectra are apparently outlines of multicomponent spectra, one can understand the nature of the plasma-induced radicals and their formation only after the spectral components have been elucidated. Thus, we have systematically conducted the computer simulations of these progressive changes of the complicated spectra in an interrelated manner.

In order to deduce the part of the component spectra, we have first obtained the difference spectra of various pairs of observed spectra among the three series of progressive spectral changes. Then, computer simulations disclosed that in the observed spectra there exist as many as six component spectra, and all the simulated spectra are obtained from admixtures of the selected component spectra with differing ratios. The simulated spectra are shown in Figure 2.

It can be seen that all the observed spectra have been satisfactorily reproduced by the simulated spectra shown in Figure 2. Figure 3 shows the representative spectral components of the simulated spectra: three isotropic spectra [doublets (**I**), triplets (**II**) and (**III**)] and three anisotropic spectra [doublet (**IV**), doublet of doublets (**V**), and single broad line (**VI**)]. For anisotropic spectra, the principal patterns of *g* factor and hyperfine splitting are also illustrated in Figure 3. The ESR spectroscopic parameters for a representative selection of these component spectra deduced from the systematic simulation are summarized in Table I. The principal anisotropic parameters somewhat vary with the

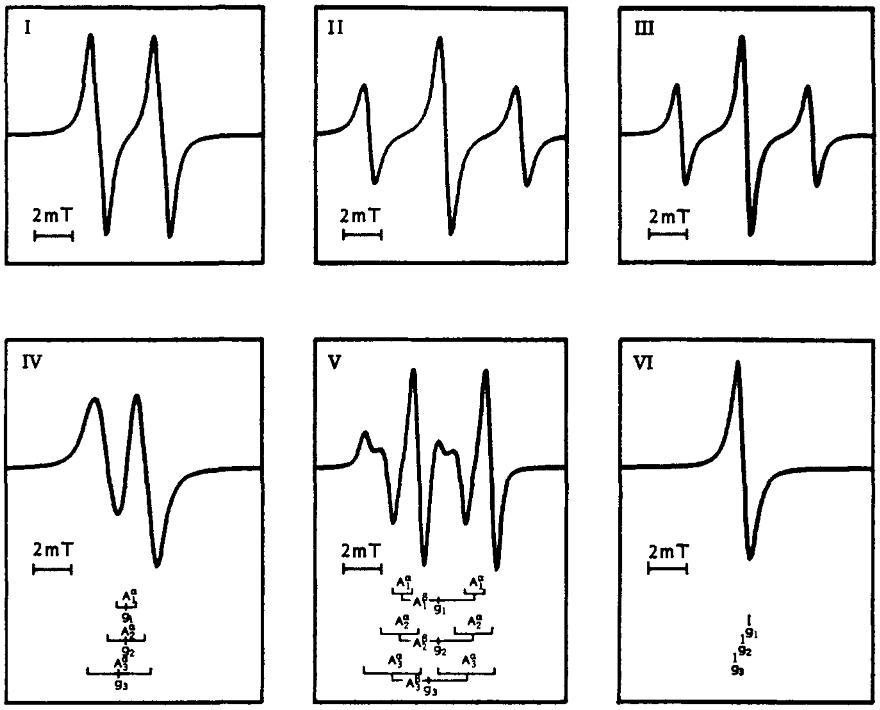

Figure 3. Six component spectra for the simulated ESR spectra. In principal pattern for IV, the small effect of β-hydrogen is not shown (see Table I).

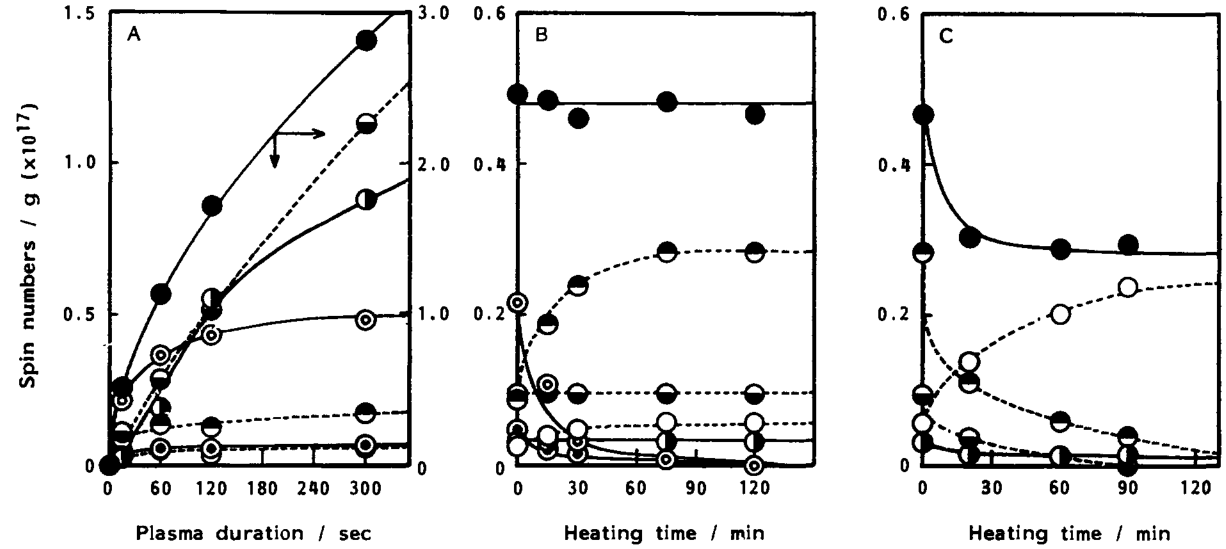

Figure 4. Progressive changes of spectral intensities of component spectra as a function of (A) plasma duration, (B) heating at 120 °C of 15-s plasma-irradiated *myo*-inositol, and (C) heating at 155 °C after heating at 120 °C for 2 h: (●) total, (◑) I, (◎) II, (⊚) III, (⊖) IV, (⊜) V, and (○) VI.

Table I. ESR Spectral Data for Component Radicals in Simulated Spectra[a]

	I	II	III	IV		V		VI	
g	2.0059	2.0025	2.0042	$\bar{g}$ = 2.0048	g_1 = 2.0042 g_2 = 2.0042 g_3 = 2.0061	$\bar{g}$ = 2.0054	g_1 = 2.0045 g_2 = 2.0045 g_3 = 2.0073	$\bar{g}$ = 2.0061	g_1 = 2.0042 g_2 = 2.0070 g_3 = 2.0073
A_α				$\bar{A}_\alpha$ = 1.88	A_1 = 1.27 A_2 = 1.70 A_3 = 2.67	$\bar{A}_\alpha$ = 1.89	A_1 = 1.00 A_2 = 1.57 A_3 = 3.11		
$A_\beta(1)$	3.08	4.13	3.45	$\bar{A}_\beta$ = 0.52	A_1 = 0.52 A_2 = 0.52 A_3 = 0.52	$\bar{A}_\beta$ = 3.83	A_1 = 3.83 A_2 = 3.83 A_3 = 3.83		
$A_\beta(2)$	0.42	4.13	3.45						

[a] Values of HSC are given in mT.

spectra so that their values are only of semiquantitative significance.

ESR Kinetics. Figure 4 shows the progressive changes of each component spectral intensity as a function of plasma duration (A), heating time at 120 °C (B) and at 155 °C (C).

It is seen from Figure 4A that the spectra of the plasma-irradiated sample consist of six component spectra. It is apparent that the rate of increase in each spectral intensity varies with

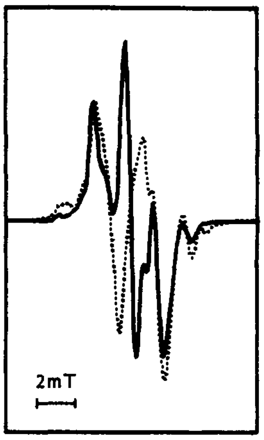

Figure 5. ESR spectrum of 300-s plasma-irradiated *myo*-inositol heated at 130 °C for 10 h. The spectrum shown as dotted line is an intermediate level of conversion.

component spectra, accounting for rather large spectral changes in the pattern in the course of plasma irradiation. The formation of two triplets (II) and (III) and doublet of doublets (V) tend to level off, although the initial rate of the formation of II is quite large, and the rest of spectra exhibit a continuous increase in intensity, indicating that they are thermally stable (vide infra).

One of the interesting features seen in Figure 4B is that the total spectral intensities remain nearly unchanged on heating at 120 °C for 2 h (in accord with the result from the doublet integration). This indicates that the major pathway at 120 °C is a radical–radical rearrangement, not a termination reaction leading to stable diamagnetic molecules. It is also seen from Figure 4B that two kinds of triplets (II) and (III) decrease in intensity and completely disappeared in 2 h, leading to the spectrum consisting of four kinds of component spectra, while the spectral intensity of a doublet of doublets (V) and single broad line (VI) increases. However, two component spectra of doublets (I) and (IV) persist nearly unchanged in intensity even on heating at 120 °C. Accordingly, it is clear that both triplets (II) and (III) must have been thermally converted to a doublet of doublets (V). This fact also indicates that the presence of V in the spectra of plasma-irradiated *myo*-inositol has resulted from thermal effect of plasma irradiation.

The nature of the component spectral changes similar to the above was also obtained by additional heating experiment of 300-s plasma-irradiated sample. As shown in Figure 5, prolonged heating of such a sample at 130 °C caused the reduction of component spectra; the triplet (II) has first dissipated followed by III and finally gave the spectrum that consists of single broad line (VI), two doublets (I and IV), and doublet of doublets (V) with the ratios of *ca.* 35:20:40:5 based on the simulation using the same component spectra as in the case of those shown in Figure 2.

It is seen from Figure 4C that heating at 155 °C caused the decrease in total spectral intensity, accompanied by the increase in the spectral intensity of single broad line (VI). Since two triplets (II) and (III) have completely dissipated at 120 °C for 2 h, the single broad line (VI) can be considered to result from the spectra of IV and V. However, the increase in the spectral intensity of VI corresponds to only ca. 40% of the decrease in the total spectral intensity during the course of heating at 155 °C for 90 min, thus indicating that IV and V have been converted not only to VI but also to nonradical species.

From the results of these systematic ESR kinetics based on the simulated spectra, the overall spectral changes can be analyzed and summarized in Scheme I.

It should be mentioned here that most of polymer radicals produced by high energy radiation[20] including plasma irradiation[9] and mechanical fracture of polymers (mechanoradicals)[21] are rapidly converted, in contact with oxygen, into the corresponding peroxy radicals. The present radicals in *myo*-inositol, however, were found to be stable in dry atmosphere at room temperature for a long period of time, and the radicals were not converted to the peroxy radicals, as in the case of most carbohydrate radicals except for polycarbohydrates.[22]

Scheme I

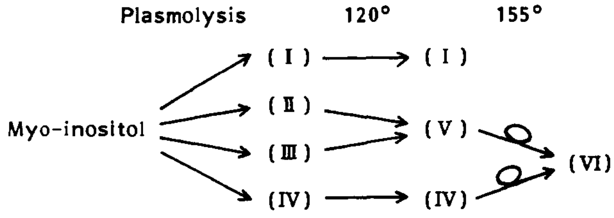

Scheme II

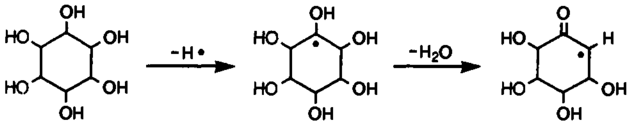

Structural Assignment. It is a well-known fact that hydrogen abstraction from a variety of alcohols including carbohydrates occurs at the carbon bearing hydroxyl groups to give hydroxylalkyl radicals not only as a radiation effect but also in chemical oxidation and photochemical reactions.[24] The resulting hydroxylalkyl radicals are also known to undergo the dehydration to give the corresponding acylalkyl radicals when the β-hydroxyl groups are present, which occurs in either acid- and base-catalyzed or uncatalyzed (thermal) conditions.[24]

In fact, the ESR spectral feature of the present radicals formed by plasma irradiation followed by temperature annealing clearly indicates that such reactions have occurred as shown in Scheme II.

However, the above reaction scheme is apparently oversimplified for the reaction of solid state *myo*-inositol. A structure of *myo*-inositol has σ-plane (C_v symmetry), and the C-2 hydrogen lies in an approximate plane (equatorial), and the rest of five hydrogens are axial so that carbon pairs, C1 vs C3 and C4 vs C6, are identical to each other. Thus, we have only to consider four possible hydroxylalkyl radicals **1**, **2**, **3**, and **7** resulting from hydrogen abstraction (diastereomers cannot be discriminated by ESR), as shown in Figure 6.

It is well-known that the HSC of β-hydrogens of alkyl radicals can be effectively described by the cosine square rule, which can be expressed as $A^{\beta}_{\mathrm{H}} = Bq \cos^2 \theta$, where θ is the angle between the H–C–C plane and the axis of p-orbital of the free electron, *B* is a proportionality constant, and *q* is a spin density of the radical center.

The spin density of the hydroxylalkyl radicals on each carbon atom in *myo*-inositol does not vary much,[26a] so that the hydroxylalkyl radical at C1(=C3) should give an apparent doublet with

---

(20) Kamachi, M. *Adv. Polym. Sci.* **1987**, *82*, 207.

(21) Kuzuya, M.; Kondo, S.; Noguchi, A.; Noda, N. *J. Polym. Sci., Polym. Phys. Ed.* **1992**, *30*, 97.

(22) We have already undertaken plasma irradiation on a number of carbohydrates including mono-, oligo-, and polycarbohydrates, whose results are reported later elsewhere. It has been shown that the radicals formed were very stable in dry atmosphere. It is apparent that oxygen under atmospheric pressure cannot diffuse into the hydrogen bonding network of carbohydrates.[23]

(23) Ueda, H.; Kuri, Z.; Shida, S. *Nippon Kagaku Kaishi* (*Jpn.*) **1961**, 82.

(24) (a) Livingston, R.; Zeldes, H. *J. Chem. Phys.* **1966**, *44*, 1249. (b) Buley, A. L.; Norman, R. O. C.; Pritchett, R. J. *J. Chem. Soc.* (*B*) **1966**, 849. (c) Steenken, S.; Davies, M. J.; Gilbert, B. C. *J. Chem. Soc., Perkin Trans. 2*, **1986**, 1003.

(25) It has been shown, in fact, that this type of reaction has occurred as a major process in all plasma-irradiated carbohydrates.[22]

(26) (a) This was confirmed by the molecular orbital calculations (the UAM1 method). The calculated π-spin densities (ρ) of the equilibrium geometry were as follows: $\rho1(\rho3) = 0.796$, $\rho2 = 0.800$, $\rho4(\rho6) = 0.795$, $\rho5 = 0.801$. (b) According to the cosine square rule, the HSC of an equatorial β-hydrogen can be deduced to be 0.5–0.6 mT from the equilibrium geometry for **7** (*ca.* 66° for θ), taking the calculated spin density as well as the value of 4.5 mT for B.

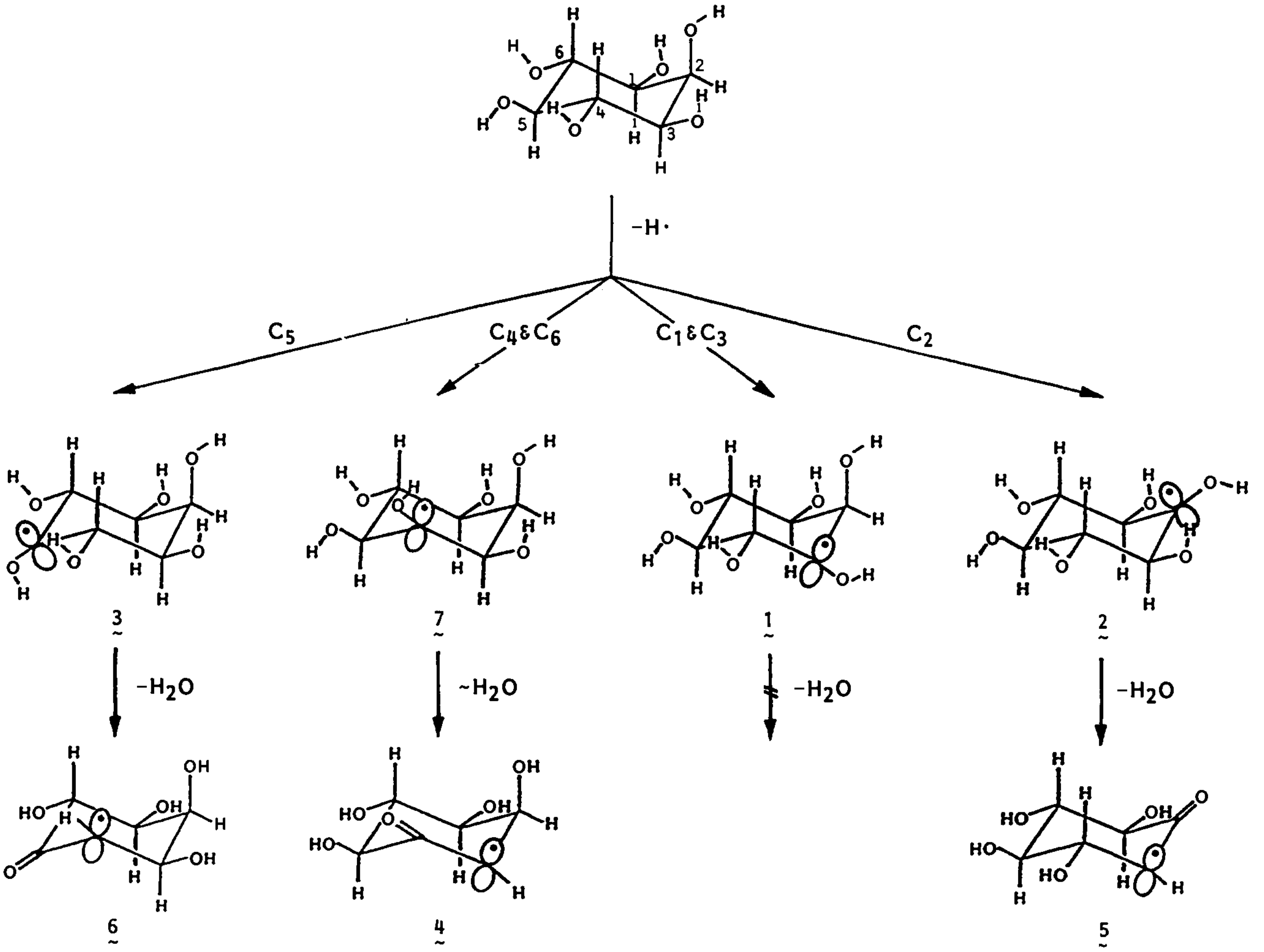

Figure 6. Structures of *myo*-inositol radicals and the reaction sequence.

the splitting of one β-hydrogen in the ESR spectrum, since the C-2 hydrogen is equatorial. Thus, as shown in Figure 6, the stable doublet (I), with the HSC of ca. 3.1 mT, can be unambiguously assigned to the hydroxylalkyl radical at C1(=C3) (**1**), among the four possible hydroxylalkyl radicals. Likewise, we can assign the doublet (IV) with *g* factor and hyperfine anisotropy to the acylalkyl radical at C1(=C3) (**4**), which must have resulted from the dehydration of hydroxylalkyl radical at C4(=C6) (**7**).[26b] It is apparent that the *g* factor anisotropy and hyperfine anisotropy of **4** is caused by carbonyl conjugation and the presence of α-hydrogen. The amount of α-hydrogen hyperfine anisotropy (A_3–A_1) as well as the isotropic value ($\bar{A}_\alpha$) (Table I) is compatible with those of various carbonyl-conjugated alkyl radicals.[27] Thus, the A_3 and A_1 should correspond to in-plane direction perpendicular to the C–H bond and along the C–H bond, respectively.

It should be mentioned that there are two plausible pathways for **7** to undergo the dehydration with the hydroxyl group either at C3(=C1) or C5. However, based on the fact that the acylalkyl radical (**4**) is present even at the early stage of plasma irradiation (15-s plasma duration) and the spectral intensity of such a radical (**4**) did not increase on heating at 120 °C (Figure 4B), it is reasonably assumed that hydroxylalkyl radical (**7**), precursor of **4**, does not exist at any stage of the spectral changes, but **7** was very susceptible to thermal dehydration with the β-hydroxyl group at C3(=C1) to give **4**. This anomaly will be further discussed later including the stability of hydroxylalkyl radical (**1**). Furthermore, based on the rationale given later, the triplets (II) and (III) are assigned to hydroxylalkyl radicals at C2 (**2**) and at C5 (**3**), respectively. Then, from the sequence shown in Scheme I, a doublet of doublets (V) should be assigned to the acylalkyl radicals at C1(=C3) (**5**) and at C4(=C6) (**6**). The nature of the anisotropy of *g* factor and hyperfine interaction in the spectrum (V) is similar to that of IV but differs in large isotropic splitting at each axis due to the presence of an axial β-hydrogen (Table I).

Finally, although the single broad line (VI) was represented by a singlet with a small amount of *g* anisotropy, and the isotropic *g* value ($\bar{g}$) indicates that it is a carbon-centered, not oxygen-centered, radical, we cannot present any discrete radical structure for VI. This radical may be a mixture of ring-opened and/or conjugated structure and of no structural significance. All these structural assignments and the reaction sequence are shown in Figure 6.

On the basis of the overall structural assignments given above and the ESR kinetics (Figure 4), it can be concluded that the hydroxylalkyl radical formation is most favorable at C2 and C5. The initial rate of the hydrogen abstraction deduced from Figure 4A is ca. 25.5 for C2 and C5, ca. 6.9 for C1(=C3), and ca. 6.3 for C4(=C6) (spin numbers $\times 10^{14}$ g/s).

We also note that hydroxylalkyl radical (**2**) is more prone to undergo the dehydration than **3**, based on the result of the heating experiment shown in Figure 5 (vide infra).

Spin Trapping Reaction. In order to scrutinize the above-mentioned structural assignments, we have also performed the spin trapping reaction of *myo*-inositol sample plasma-irradiated for 3 min, as a representative example, in benzene solution containing 2,4,6-tri-*tert*-butylnitrosobenzene (BNB) as a spin trap, according to the procedure similar to that previously reported.[21,28]

As shown in Figure 7A, the ESR spectrum of spin adducts was obtained on standing of the solution for 1 h at room temperature, apparently exhibiting outlines of multicomponent spectra.

The computer simulated spectra shown in Figure 7B together with the component spectra disclosed that the observed spectrum

---

(27) See, for example: Lefebvre, R.; Maruani, J. *J. Chem. Phys.* **1965**, *42*, 1480.

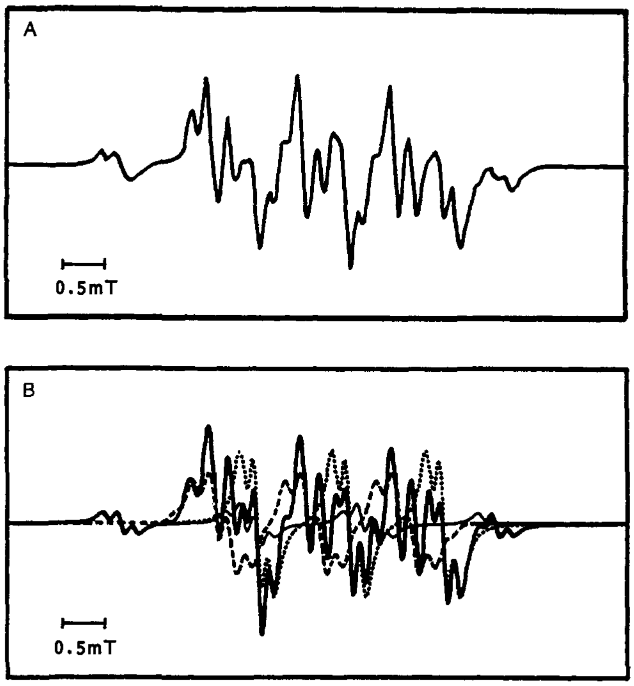

Figure 7. ESR spectrum of BNB spin adducts: (A) observed spectrum and (B) simulated spectrum together with the component spectra (···) a triplet of triplets (a), (- -) a quartet of triplets (b), (—) a doublet of triplets (c).

can be approximated essentially by three kinds of component spectra, a triplet of triplets (a), a quartet of triplets (b), and a doublet of triplets each component peak being further split to a triplet with 0.15 mT (c), with the ratio of 44:44:12. Each spectral feature as well as the value of g factor and HSC [$g = 2.0028$, $a_N = 1.039$ mT, $a_{H_{arom}}$ (2) = 0.144 mT for (a), $g = 2.0053$, $a_N = 1.022$ mT, $a_H = a_{H_{arom}}$ (2) = 0.194 mT for (b), and $g = 2.0056$, $a_N = 1.325$ mT, $a_H = 1.495$ mT, $a_{H_{arom}}$ (2) = 0.15 mT for (c)] is typical for a BNB spin adduct (alkoxyl anilino radicals) trapped by tertiary alkyl radicals and bulky secondary alkyl radicals and nitroxide radical trapped by secondary hydroxylalkyl radicals, respectively.[29]

Thus, the ratio of the spin adduct trapped by secondary and tertiary radicals (ca. 56:44) was in reasonable agreement with the one estimated from the kinetic's curves (at 120-s irradiation) shown in Figure 4A [ca. (I + II + III):(IV + V) = 59:41], reinforcing the result of the assignments.

Discussion

On the basis of the structural assignment described above, we have obtained several intriguing facts to discuss, especially on the anomalous behaviors of hydroxylalkyl radicals such as the stability of **1** and high reactivity of **7** to give **4** exclusively between the two possible pathways for the dehydration.

We note that the above anomalies are apparently associated with reactions involving the hydroxyl group of *myo*-inositol at C1(=C3). If one does not consider the further detailed crystal structure of *myo*-inositol including the conformation of a hydroxyl group, there is no obvious reason why the hydroxyl group at C1(=C3) would affect the reactivity (stability) of the radicals.

Importance of the hydrogen-bonding network has often been emphasized to understand the nature of radical formation of solid state carbohydrates. For instance, it has been shown that the hydrogen bonding scheme is important for the selective formation of radicals in organic crystals.[30,31] The hydrogen atom in the shortest hydrogen bond is the easiest to abstract.[31] In fact, the preferential hydrogen elimination at C2 and C5 in *myo*-inositol observed by plasma irradiation may be rationalized in terms of consideration of an asymmetric unit of two molecules in the hydrogen bonding scheme of anhydrous *myo*-inositol (Figure 8). However, little attention has been paid to such a detailed extent as the conformation of the hydroxyl group in the hydrogen bonding scheme of the crystalline structure.[32]

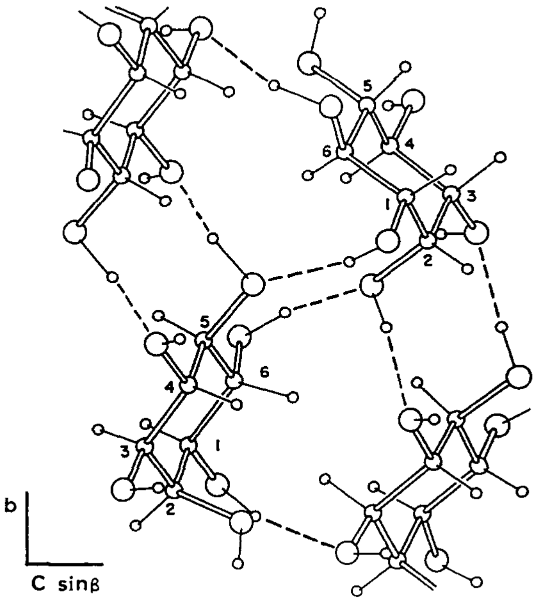

Figure 8. Crystal structure of the asymmetric unit of anhydrous *myo*-inositol, cited from ref 33.

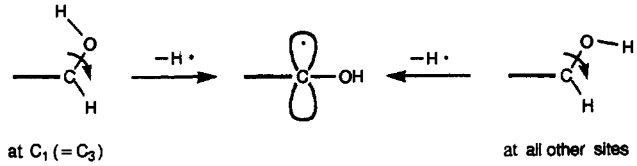

Figure 9. Schematic view of hydroxyl group motion for the formation of hydroxylalkyl radicals by hydrogen abstraction at C1(=C3) and at all other sites of *myo*-inositol.

Figure 8 shows the crystal structure of the asymmetric unit of anhydrous *myo*-inositol projected along the *a* axis determined by Rubinowitz and Kraut.[33]

One of the special features in the crystal structure of *myo*-inositol shown in Figure 8 is the fact that only the hydrogen atom of hydroxyl group at C1(=C3) carbon is *s*-trans to the one attached to the same carbon with respect to the C–O bond axis, while all other hydrogens are *s*-cis (see also the uppermost structure in Figure 6).

In fact, the observed anomalies can best be understood if one takes the specific feature of the hydrogen-bonding scheme associated with the conformational difference in the O–H bond direction at C1(=C3) into consideration. Our interpretations are as follows.

1. Stability of Hydroxylalkyl Radical (1). Formation of organic free radicals by elimination reactions is accompanied by an orbital rehybridization from tetrahedral sp^3 carbon to planar sp^2 carbon center in most cases. Thus, in order to furnish the rehybridization on the formation of hydroxylalkyl radical (**1**) by hydrogen abstraction on crystalline *myo*-inositol, the hydroxyl group at C1(=C3) should be shifted to the direction indicated by the arrow in Figure 9, contrary to the direction of hydroxyl groups at all other carbons.

---

(28) Kuzuya, M.; Nakai, S.; Okuda, T.; Kawaguchi, T.; Yanagihara, Y. *J. Chem. Soc., Faraday Trans. 1* **1987**, *83*, 1579.

(29) Terabe, S.; Konaka, R. *J. Chem. Soc., Perkin Trans. 2* **1973**, *2*, 368.

(30) Toriyama, K.; Iwasaki, M. *J. Am. Chem. Soc.* **1979**, *101*, 2516.

(31) Minakata, K.; Iwasaki, M. *J. Chem. Phys.* **1972**, *57*, 4758.

(32) For reactions in aqueous solution, it has been demonstrated that the dehydration from the hydroxylalkyl radical is more feasible when the β-hydroxyl group is eclipsed to the orbital of unpaired electron (with axial β-hydroxyl group), which should be considered distinct in nature from the reactions with rigid hydroxyl conformation in the crystalline states.[24c]

(33) Rabinowitz, I. N.; Kraut, *J. Acta. Cryst.* **1964**, *17*, 159.

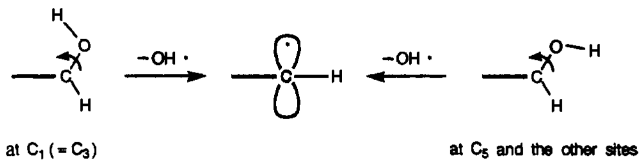

Figure 10. Schematic view of hydroxyl group motion for the formation of acylalkyl radicals by elimination of hydroxyl group at C1(=C3) and at all other sites of *myo*-inositol.

Figure 9 embodies several important features. The shift of hydroxyl group of C1(=C3) carbon of crystalline *myo*-inositol retaining the original conformation[34] would bring about a weakening of the intermolecular hydrogen bond at C1(=C3) more than at any other site due to a much larger shift of the hydrogen atom at C1(=C3) from the original position. Since the hydrogen bonds exist along the O–H bond axis (Figure 8), this makes essentially the hydroxyl group at C1(=C3) isolate from the hydrogen bonding network, necessarily resulting in strengthening (shortening) of the O–H bond at the C1(=C3) carbon. Since the dehydration of hydroxylalkyl radical to the acylalkyl radical involves the cleavage of O–H bond of the α-hydroxyl group, the above feature could suppress the dehydration process to a great extent. We believe this is the essential reason for the observed stability of the hydroxylalkyl radicals at C1(=C3) (**1**) in the crystalline state.

2. Site Specificity of Thermal Dehydration of 7. In order for **7** to give acylalkyl radical (**4**), the β-hydroxyl group at C3(=C1) of **7** must be eliminated, concerted with the hydrogen of α-hydroxyl group on the radical center at C4(=C6). In this event, as the dehydration proceeds, hydrogen-bonded β-hydroxyl groups must be removed from C3(=C1) carbon presumably toward the direction indicated by arrow in Figure 10, in order to furnish the effective orbital rehybridization from tetrahedral sp^3 carbon to planar sp^2 carbon.

As is illustrated in Figure 10 together with the elimination mode of another carbon at C5, it is conceptionally similar to that of Figure 9 but in a reverse fashion with respect to the hydroxyl group.

Preliminary molecular orbital calculations by the UAM1 method for elimination of the hydroxyl group from two isomeric methanols, *s*-trans and *s*-cis, as the simplest model compounds on the reaction mode shown in Figure 10 have indicated that elimination of the hydroxyl group from *s*-trans methanol [corresponding to C3(=C1) in *myo*-inositol] is energetically more feasible than *s-cis*-methanol (corresponding to C5 and the other carbons) by ca. 2 Kcal/mol, accompanying the lengthening of the C–O bond distances with the orbital rehybridization of methanol carbon toward the planar sp^2 carbon.

Furthermore, the hydrogen bond would be maintained until near completion of the elimination of the hydroxyl group at C3(=C1), while such a hydrogen bond would be disrupted at a rather earlier stage of dehydration with the hydroxyl group at C5. It can be considered, therefore, that the nature of hydrogen bond could further enhance the difference in reactivity between the two isomeric hydroxyl groups.

This kind of interpretation based on the specific hydroxyl conformation at C1(=C3) also concomitantly accounts for more facile formation of the acylalkyl radical (**5**) from hydroxylalkyl radical at C2 (**2**) than that of **6** from **3** (vide supra), since the dehydration of **2** also involves the elimination of the β-hydroxyl group at C1(=C3).

Thus, all special features observed could be explained under the consideration of special conformation of the hydroxyl group at C1(=C3) in the crystalline state, and it seems otherwise difficult to interpret the observed specificities. However, we emphasize again that this kind of interpretation is valid strictly only for solid state reactions where the conformation of hydroxyl group is retained due to the hydrogen bonding network, and there exists no such a regulation of the conformation of hydroxyl group in liquid and/or gas phase where a hydroxyl group is freely rotating.

Conclusions

The conclusions drawn from the present study can be summarized as follows: We have first presented the detailed analysis of carbohydrate radicals (*myo*-inositol) generated by plasma irradiation. Combined data on the studies of the systematic ESR kinetics of plasma-induced radical formation and temperature annealing coupled with the systematic computer simulations enabled us to clarify the precise nature of radical formation in *myo*-inositol by plasma irradiation.

It was found that all possible four hydroxylalkyl radicals (**1**, **2**, **3**, and **7**) by hydrogen abstraction were formed as primary products but with a preference at C2 and C5. Among the four radicals formed, however, the radical at C4(=C6) (**7**) was unobserved, which underwent spontaneously the thermal dehydration to give the acylalkyl radical (**4**), exclusively. In contrast, the radical (**1**) was stable so that it did not undergo the thermal dehydration to an appreciable extent even at 120 °C for 2 h. Three acylalkyl radicals (**4**, **5**, and **6**) are secondary products derived from dehydration of the hydroxylalkyl radicals (**7**, **2**, and **3**, respectively), although the radicals (**5** and **6**) were not discriminated by the ESR spectrum.

All the anomalies observed have been rationalized in terms of the basis that the orbital rehybridization from tetrahedral sp^3 carbon to the planar sp^2 carbon on the radical formation has caused the difference in reactivities between the C1(=C3) carbon and the other carbons due to the special conformation of hydroxyl group at C1(=C3) in crystalline *myo*-inositol.

This kind of a pioneering concept, in principle, seems applicable to the structural identification of a wide variety of radicals in more complicated carbohydrates, if they have such hydroxyl groups in the crystal structure. In fact, the presence of *s*-trans conformation of the hydroxyl group can be found in α-anomeric isomers of many carbohydrates from inspection of available crystal structures of carbohydrates.

We believe that many investigators should benefit from such an analysis on the structural identification of solid state radicals in a variety of carbohydrates and their structurally related compounds.

---

[34] It has been shown that plasma irradiation did not disrupt the crystal structure of *myo*-inositol within a limit of detection by X-ray powder diffraction pattern measurement (Riguku RAD-1C).